



LAWRENCE
LIVERMORE
NATIONAL
LABORATORY

Preliminary Simulations of CO₂ Transport in the Dolostone Formations in the Ordos Basin, China

Y. Hao, T. Wolery, S. Carroll

May 1, 2009

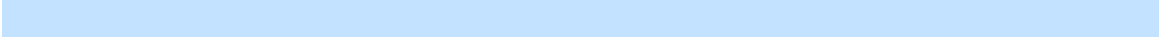
Disclaimer

This document was prepared as an account of work sponsored by an agency of the United States government. Neither the United States government nor Lawrence Livermore National Security, LLC, nor any of their employees makes any warranty, expressed or implied, or assumes any legal liability or responsibility for the accuracy, completeness, or usefulness of any information, apparatus, product, or process disclosed, or represents that its use would not infringe privately owned rights. Reference herein to any specific commercial product, process, or service by trade name, trademark, manufacturer, or otherwise does not necessarily constitute or imply its endorsement, recommendation, or favoring by the United States government or Lawrence Livermore National Security, LLC. The views and opinions of authors expressed herein do not necessarily state or reflect those of the United States government or Lawrence Livermore National Security, LLC, and shall not be used for advertising or product endorsement purposes.

This work performed under the auspices of the U.S. Department of Energy by Lawrence Livermore National Laboratory under Contract DE-AC52-07NA27344.

Preliminary Simulations of CO₂ Transport in the Dolostone Formations in the Ordos Basin, China

Yue Hao, Tom Wolery, Susan Carroll
Lawrence Livermore National Laboratory



Abstract

This report summarizes preliminary 2-D reactive-transport simulations on the injection, storage and transport of supercritical CO₂ in dolostone formations in the Ordos Basin in China. The purpose of the simulations was to evaluate the role that basin heterogeneity, permeability, CO₂ flux, and geochemical reactions between the carbonate geology and the CO₂ equilibrated brines have on the evolution of porosity and permeability in the storage reservoir. The 2-D simulation of CO₂ injection at 10³ ton/year corresponds to CO₂ injection at a rate of 3 x 10⁵ ton/year in a 3-D, low permeable rock. An average permeability of 10 md was used in the simulation and reflects the upper range of permeability reported for the Ordos Basin Majiagou Group. Transport and distribution of CO₂ between in the gas, aqueous, and solid phases were followed during a 10-year injection phase and a 10-year post injection phase.

Our results show that CO₂ flux and the spatial distribution of reservoir permeability will dictate the transport of CO₂ in the injection and post injection phases. The injection rate of supercritical CO₂ into low permeable reservoirs may need to be adjusted to avoid over pressure and mechanical damage to the reservoir. Although it should be noted that 3-D simulations are needed to more accurately model pressure build-up in the injection phase. There is negligible change in porosity and permeability due to carbonate mineral dissolution or anhydrite precipitation because a very small amount of carbonate dissolution is required to reach equilibrium with respect these phases. Injected CO₂ is stored largely in supercritical and dissolved phases. During the injection phase, CO₂ is transport driven by pressure build up and CO₂ buoyancy.

Introduction

China is increasing its emphasis on the production of hydrocarbons in addition to the development of nuclear power and renewable energy sources in order to meet its growing energy demands. Carbon storage as a liquid, gas, dissolved carbon, or as carbonate minerals has the potential to significantly offset global warming caused by anthropogenic combustion of fossil fuels (IPCC 2007, IEA 2007). It is generally accepted that the most suitable systems for geologic storage are depleted oil and deep saline reservoirs, because they are not viable for domestic, industrial, and agricultural uses and they are separated from the atmosphere by 1000s of meters of geologic strata. Geological sequestration of CO₂ to limit atmospheric emissions has been underway for more than a decade with projects that have provided significant data and experience (e.g., Sleipner in Norway, In Salah in Algeria, and a joint US-Canadian effort at the Dakota Gasification facility and Weyburn field). Numerous field projects in the United States and Canada are in development through the DOE's Regional Carbon Sequestration Partnerships program.

In this preliminary study we focus on the storage of supercritical CO₂ in dolostone formations in the Ordos Basin in China using 2-D reactive transport simulations. The purpose of the simulations was to evaluate the role that basin heterogeneity, permeability, CO₂ flux, and geochemical reactions between the

carbonate geology and the CO₂ equilibrated brines have on the evolution of porosity and permeability in the storage reservoir.

Approach

The numerical reactive-transport simulations were performed using the Nonisothermal Unsaturated-Saturated Flow and Transport code (NUFT) to handle 3-D flow and 2-D reactive flow and transport calculations (Nitao 1998). The NUFT code is a highly flexible software package for modeling multiphase, multi-component heat and mass flow and reactive transport in unsaturated and saturated porous media. An integrated finite-difference spatial discretization scheme is used to solve mass and energy balance equations in both flow and reactive transport models. The resulting nonlinear equations are solved by the Newton-Raphson method. The NUFT code is capable of running on PCs, workstations, and major parallel processing platforms. Some of the application areas include: nuclear waste disposal, CO₂ sequestration, groundwater remediation, and subsurface hydrocarbon production (Buscheck et al., 2003; Carroll et al., 2008; Glassley et al., 2003; Johnson et al., 2004, 2005).

Table 1. Geologic model used in simulations at 95°C and 300 bars.

Layers	¹ Geology	¹ Porosity (%)	² Permeability (md)	¹ Permeability (md)	² Mineralogy
1	Dolostone 5 m	5	10	1	Dolomite (98%) Calcite (1%) Anhydrite (1%)
2	Muddy dolostone 3 m	1.5	3	0.3	Dolomite (98%) Calcite (1%) Anhydrite (1%)
3	Ooidic dolostone 3 m	5	10	1	Dolomite (98%) Calcite (1%) Anhydrite (1%)
4	Lime dolostone 4 m	1.5	1	0.1	Dolomite (50%) Calcite (49%) Anhydrite (1%)
5	Vuggy dolostone 5 m	15	30	3	Dolomite (98%) Calcite (1%) Anhydrite (1%)
6	Dolostone 5 m	5	10	1	Dolomite (98%) Calcite (1%) Anhydrite (1%)

1. Data reported by Wang and Al-Aasm, 2002.

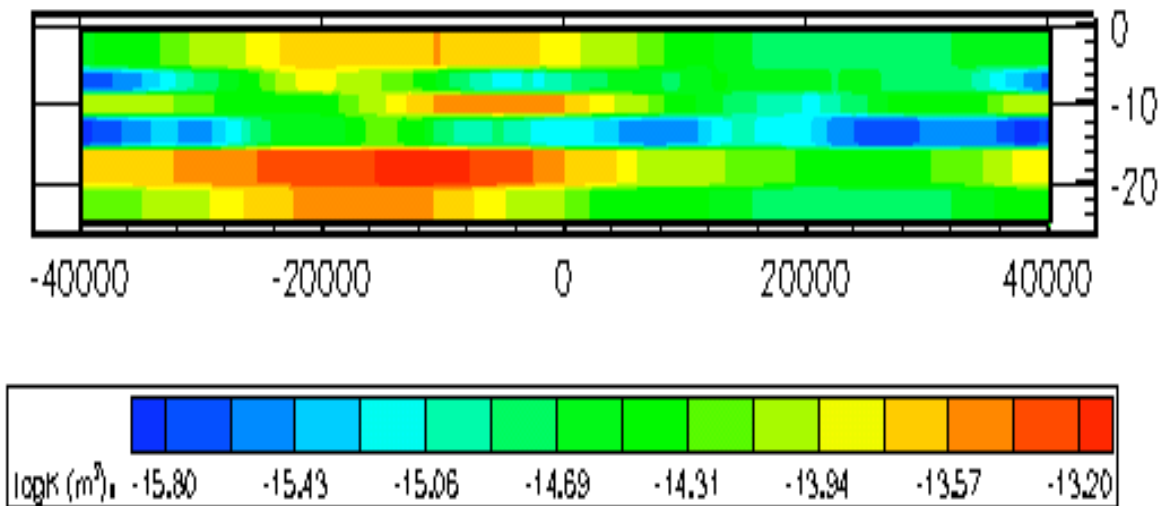


Figure 1. Vertical and horizontal heterogeneous profile used in the NUFT simulations.

Our reactive transport model is based on geochemical and physical characteristics reported for dolostones for the Ordovician Majiagou Group in the Ordos Basin, China (Wang and Al-Aasm, 2002). The hydrologic model and the permeability distributions are shown in Table 1 and Figure 1. In our simulations, supercritical CO_2 is injected into a 25 m thick dolostone group at about 3465 m below the ground surface at 95°C and 300 bars. The hydrologic model assumes that the dolostone has zero dip with no inherent hydraulic gradient. Consequently fluid flow is driven by the pressure buildup associated with the injected supercritical CO_2 only. Vertical heterogeneity is constrained by mineralogical, porosity, and permeability depth profiles. The dolostone group consists of six low permeability layers ranging from 1.5 to 15% porosity and 0.1 to 3 mD, with an average permeability of 1 mD. In our simulations we use a permeability profile that is 10 times the reported permeability, because the reported average permeability of 1 mD yields excessive pressure build up during the injection of supercritical CO_2 . This is reasonable, because an average permeability of 10 md has been reported for this formation. A fractal random field generator was used to generate the heterogeneity within each geological layer based on values in Table 1. The mineralogy of the Majiagou Group is dominated by dolomite in all layers, with the exception of layer 4, which contains about equal mixtures of dolomite and calcite. The storage interval is capped by a low permeable mudstone at the top of the reservoir and by vitric tuff at the bottom. For the purpose of this preliminary calculation, the cap rocks are assumed to non-reactive.

Injection of supercritical CO_2 into a 3-D reservoir (25 m x 80 km x 80 km) through a kilometer long horizontal pipe with 100 md permeability was simulated without reactive chemistry to estimate the maximum injection rate that would yield pressure about 150 bars above the pre-injection pressure. Simulations were extended over 6200 km^2 to appropriately model pressure gradient caused by the

CO₂ injection into low permeable geology. The 3-D permeability field simply extended the 2-D model uniformly into the third dimension.

The resulting CO₂ flux from the 3-D simulation was then scaled to 2-D for the full reactive transport simulation. Simulations of a point source injection to mimic a 2-D slice of the horizontal well resulted in abnormally low pH due to time-step issues in the numerical simulations and are not shown here. Instead we show, injection into a vertical well in the 2- slice (25 m x 50 m x 80 km). In both the 3-D and the 2-D simulations, permeability of the injection well is limited to 100 md for numerical reasons; in reality it would be much greater. CO₂ transport and reaction is tracked during an injection period of 10 years, a ramp down period of 3 months, and a post injection period of 10 years. Permeability and porosity are fixed to the initial values during the run to reduce computational expense because geochemical calculations show minimal dissolution of the carbonate geology.

The initial brine chemistry was based on the equilibration of a pH 6.5, 0.85 molal NaCl brine with dolomite, calcite, and anhydrite at 95C and 300 bars using thermodynamic constants generated by SUCRPT and the EQ3/6 reaction progress code (Wolery 1992a, Johnson et al., 1992). In the reactive transport

$$\frac{dn}{dt} = -Sk_{298.15K} e^{-E/R(T-298.15)} \left(1 - \left[\frac{Q}{K} \right] \right)$$

modeling, mineral-brine interaction was modeled using explicit kinetics instead of assuming partial equilibrium as in the EQ3/6 reaction-path calculation. Rates of interaction of a mineral with the brine were described by an equation of the form: where n is the number of moles of the mineral, t is time (s), k is the rate constant for the mineral (mol-m²-s⁻¹) at 298.15K, S is the active surface area for the mineral (m²), E is the activation energy for the mineral (kJ-mol⁻¹), T is the absolute temperature, R is the gas constant, K is the equilibrium constant for the mineral, and Q is the corresponding activity product. Here $Q = K$ implies equilibrium, $Q < K$ implies undersaturation (and dissolution), and $Q > K$ implies supersaturation (and precipitation). The rate equation was used to describe both dissolution and precipitation, with whichever process being determined by the relationship between Q and K . Note that a negative value of dn/dt indicates dissolution. The rate constants and activation energies used in this study are shown in Table 2. From the EQ3/6 calculations, quartz was expected to behave inertly, so it was not included in the set of minerals treated using a rate model.

Table 2. Kinetic rate constants for dissolution/precipitation

Mineral	log k*	E**	Source
Calcite	-5.81	23.5	Palandri and Kharaka (2004)
Dolomite	-7.53	52.2	Palandri and Kharaka (2004)
Magnesite	-9.34	23.5	Palandri and Kharaka (2004)
Anhydrite	-3.19	14.3	Palandri and Kharaka (2004)

*dissolution rate constant at 298.15°K, consistent with units of mol-m²-s⁻¹

**activation energy, kJ-mol⁻¹

Results and Discussion

The simulations suggest that CO₂ is largely confined to the supercritical and aqueous phases, and that transport is dependent both on CO₂ buoyancy and reservoir permeability magnitude and distribution. Negligible changes in porosity and permeability result from the reaction of the supercritical CO₂, because very little calcite or dolomite dissolves to reach equilibrium.

Simulation of Brine Chemistry

Specific compositional data for formation brines in the Ordovician dolomite unit and surrounding units in the proposed injection area are not available. The actual formation brine in these units is probably NaCl dominated with overall concentrations roughly equivalent to 0.7 m NaCl (similar to seawater) to 3 m NaCl. For the present calculations, we have chosen a composition slightly more concentrated than seawater, but less than the 1.0 m ionic strength limit commonly associated with the “B-dot” model for activity coefficients (Helgeson, 1969). To model the brine accurately at higher ionic strength would require a high-temperature Pitzer model such as that of Greenberg and Møller (1989), but extended to incorporate pressure dependence. The target formation is known to contain mainly dolomite [CaMg(CO₃)₂], here represented as “Dolomite-ord” or ordered dolomite, with calcite (CaCO₃) as a major component in one sub-unit. Anhydrite (CaSO₄) and quartz are likely present at some level, in the caprock if not the target formation.

A hypothetical working brine composition was developed using the EQ3/6 geochemical modeling software (Wolery, 1992a). For modeling purposes, the temperature is taken to be 95°C and the total pressure is 300 bars. To construct the brine, the Na⁺ and Cl⁻ concentrations were set to 0.85 molal, and the K⁺ was set to 0.012 molal. These are thought to be reasonable values for a deep formation brine in the chosen target composition range. Ca²⁺ was calculated by assuming equilibrium with calcite, Mg²⁺ by equilibrium with dolomite-dis (disordered dolomite), SO₄²⁻ by equilibrium with anhydrite, and SiO_{2(aq)} by equilibrium with quartz. HCO₃⁻ was adjusted from a starting value of 0.01 molal to satisfy electrical balance. The software SUPCRT92 (Johnson et al., 1992) was used to generate accurate 300 bar data for use both in EQ3/6 and NUFT, and the EQ3NR. The SUPCRT92 data (calculated using a modified form of the slop98.dat database distributed on the Everett Shock website) pertinent to the formation temperature and pressure are given in Table 3. Magnesite (MgCO₃) was included because it was closer to saturation in the model brine than any other mineral that might possibly form as a new product phase. Kinetically, it is somewhat unlikely that either dolomite or magnesite would be able to precipitate in the formation following the injection of CO₂.

The calculated ambient (initial) brine composition is given in Table 4. The assumed mineral equilibria only slightly add to the load of dissolved components. The brine is still dominated by sodium chloride. This composition was then used to initialize the ambient brine in the NUFT calculations.

Table 3. Reactions for hypothetical Ordos Basin (Ordovician unit) brine. Temperature is 95°C and the pressure is 300 bars.

Reaction	log K
Dolomite-ord + 2 H ⁺ = Ca ²⁺ + Mg ²⁺ + 2 HCO ₃ ⁻	0.4777
Calcite + H ⁺ = Ca ²⁺ + HCO ₃ ⁻	0.9697
Anhydrite = Ca ²⁺ + SO ₄ ²⁻	-5.0872
Quartz = SiO _{2(aq)}	-3.0071
Magnesite + H ⁺ = Mg ²⁺ + HCO ₃ ⁻	0.7980
NaCl _(aq) = Na ⁺ + Cl ⁻	0.5337
CaSO _{4(aq)} = Ca ²⁺ + SO ₄ ²⁻	-2.4304
CaCl ⁺ = Ca ²⁺ + Cl ⁻	-0.1385
CO _{2(aq)} + H ₂ O = H ⁺ + HCO ₃ ⁻	-6.2439
KSO ₄ ⁻ = K ⁺ + SO ₄ ²⁻	-1.1494
KCl _(aq) = K ⁺ + Cl ⁻	1.8390
CaCl _{2(aq)} = Ca ²⁺ + 2 Cl ⁻	0.5246
CaHCO ₃ ⁺ = Ca ²⁺ + HCO ₃ ⁻	-1.3440
MgCl ⁺ = Mg ²⁺ + Cl ⁻	-0.1082
NaHSiO _{3(aq)} + H ⁺ = Na ⁺ + SiO _{2(aq)} + H ₂ O	7.6693
CaCO _{3(aq)} + H ⁺ = Ca ²⁺ + HCO ₃ ⁻	5.9441
MgHCO ₃ ⁺ = Mg ²⁺ + HCO ₃ ⁻	-1.3513
HSiO ₃ ⁻ + H ⁺ = SiO _{2(aq)} + H ₂ O	8.8690
OH ⁻ + H ⁺ = H ₂ O	12.2384
CO ₃ ²⁻ + H ⁺ = HCO ₃ ⁻	9.9340
HSO ₄ ⁻ = H ⁺ + SO ₄ ²⁻	-2.8355
NaOH _(aq) + H ⁺ = Na ⁺ + H ₂ O	12.4061
MgCO _{3(aq)} + H ⁺ = Mg ²⁺ + HCO ₃ ⁻	6.5392
KHSO _{4(aq)} = K ⁺ + H ⁺ + SO ₄ ²⁻	-0.2031
CO _{2(g)} + H ₂ O = H ⁺ + HCO ₃ ⁻	-8.3463

Table 4. Composition of hypothetical Ordos Basin (Ordovician unit) brine. See text for details.

Component	mg/L	Molality
Ca ²⁺	832.22	0.0207651
Cl ⁻	30135	0.85
HCO ₃ ⁻	134.53	0.0022048
K ⁺	469.18	0.012
Mg ²⁺	11.784	0.0004849
Na ⁺	19541	0.85
SO ₄ ²⁻	2532.2	0.0263599
SiO _{2(aq)}	60.876	0.0010132
pH	---	6.5*
Ionic strength	---	0.871157
*unitless		

Prior to making the NUFT calculations, the overall effect of adding CO₂ to the target formation was assessed using the EQ6 reaction-path code (Wolery and Daveler, 1992). The purpose was to gain insight on the fundamental geochemical processes in the absence of transport effects, and to ensure that the introduction of CO₂ while maintaining partial equilibrium (or near-partial equilibrium) with the initially present formation minerals would not introduce new and unanticipated effects, such as the formation of additional minerals or aqueous species that would require additional thermodynamic data.

The calculated modified brine (taken to a CO₂ pressure of 300 bars, matching the expected ambient initial pressure) is represented in Table 5. The pH has dropped significantly, from 6.5 to 4.55. The “HCO₃⁻” component has increased to about 2.0 molal. Most of this is actually in the form of the species CO_{2(aq)}, as is shown in Table 4. Note that, over pressure would increase dissolved CO₂ and lower the pH somewhat further. It should be noted that although the HCO₃⁻ species is small in comparison to CO_{2(aq)}, it increased over the ambient value.

Table 5. Composition of hypothetical Ordos Basin (Ordovician unit) brine, calculated using the EQ6 reaction path code. The original brine is modified by adding CO₂ to raise the CO₂ pressure to 300 bars, while maintaining partial equilibrium with Dolomite-dis, Calcite, Anhydrite, and Quartz. Temperature is 95°C, and the total pressure is 300 bars.

Component	mg/L	Molality
Ca ²⁺	1690.2	0.0482853
Cl ⁻	26339	0.8506129
HCO ₃ ⁻	108910	2.0435967
K ⁺	410.08	0.0120087
Mg ²⁺	27.197	0.0012812
Na ⁺	17080	0.8506129
SO ₄ ²⁻	1236.0	0.0147321
SiO _{2(aq)}	51.160	0.0009749
pH	---	4.5519*
Ionic strength	---	0.920694
*unitless		

Table 6. Mineral dissolution/precipitation and speciation of the HCO_3^- component of modified hypothetical Ordos Basin (Ordovician unit) brine, calculated using the EQ6 reaction path code. The original brine is modified by adding CO_2 to raise the CO_2 pressure to 300 bars, while maintaining partial equilibrium with Dolomite-dis, Calcite, Anhydrite, and Quartz. Temperature is 95°C , and the total pressure is 300 bars.

Species	Molality	Percentage
$\text{CO}_{2(\text{aq})}$	1.9619	96.00
HCO_3^-	0.072121	3.53
Subtotal	2.0340	99.53

Minerals	Moles dissolved per kg of initial solvent H_2O^*	Moles precipitated per kg of initial solvent H_2O^*
Dolomite-dis	5.08×10^{-8}	---
Calcite	1.78×10^{-6}	---
Anhydrite	---	1.00×10^{-5}
Quartz	---	1.00×10^{-6}

*Final solvent H_2O mass was 0.99928 kg.

Table 6 summarizes the net dissolution/precipitation of these minerals and the carbonate speciation when supercritical CO_2 is reacted with a hypothetical Ordos Basin brine and carbonate geology. Overall, the injection of CO_2 is not likely to cause much modification of the target formation rock, because a very small amount of mineral dissolution and precipitation is sufficient to maintain equilibrium with the minerals initially present. In the presence of transport (groundwater flow), increased dissolution/precipitation could occur in a given location due to the introduction of more ambient brine (assuming enough injected CO_2 remains at the location). During this reaction path calculation, small amounts of dolomite and calcite dissolved, the amount of anhydrite slightly increased (owing to the availability of Ca^{2+} , mainly from the dissolution of calcite), and the amount of quartz barely changed (a small amount precipitated). No new minerals formed in this simulation.

3-D Simulation

Successful storage of supercritical CO_2 requires that pressure generated during the injection of the CO_2 into the reservoir not fracture the cap rock that is meant to seal the CO_2 in place. This is especially important for low permeability rocks such as those Ordovician Majiagou Group in the Ordos Basin, China, the rate at which CO_2 can be distributed within the geologic formation will be limited by the permeability. In our simulations, we found that an injection of CO_2 equal to 3×10^5 tons/year into a geologic formation with an average permeability of 10 md (Figure 1) yields an over pressure of about 120 bars within the vicinity the injection well. The pressure then grades to ambient or pre-injection pressure from the injection well towards the boundary at 40 km. A flux of CO_2 equal to $3 \times$

10^5 tons/year is on the order of the amount of CO_2 that is currently being injected at the Krechba carbon sequestration site, in Salah, Algeria. The CO_2 storage reservoir at Krechba consists of low permeable sandstone formation. Similar pressure gradients are achieved in 2-D with a CO_2 injection flux of 10^3 tons/year. Figure 2 compares the pressure fields after 10 years of injection for 2-D and 3-D simulations, when CO_2 is injected at 3×10^5 into a 3-D reservoir (25 m x 80 km x 80 km) and at 10^3 ton/year into the 2-D reservoir (25 m x 50 m x 80 km). In the following 2-D reactive transport simulations we use a CO_2 injection equal to 10^3 ton/year as a model of what would occur in a commercial scale operation.

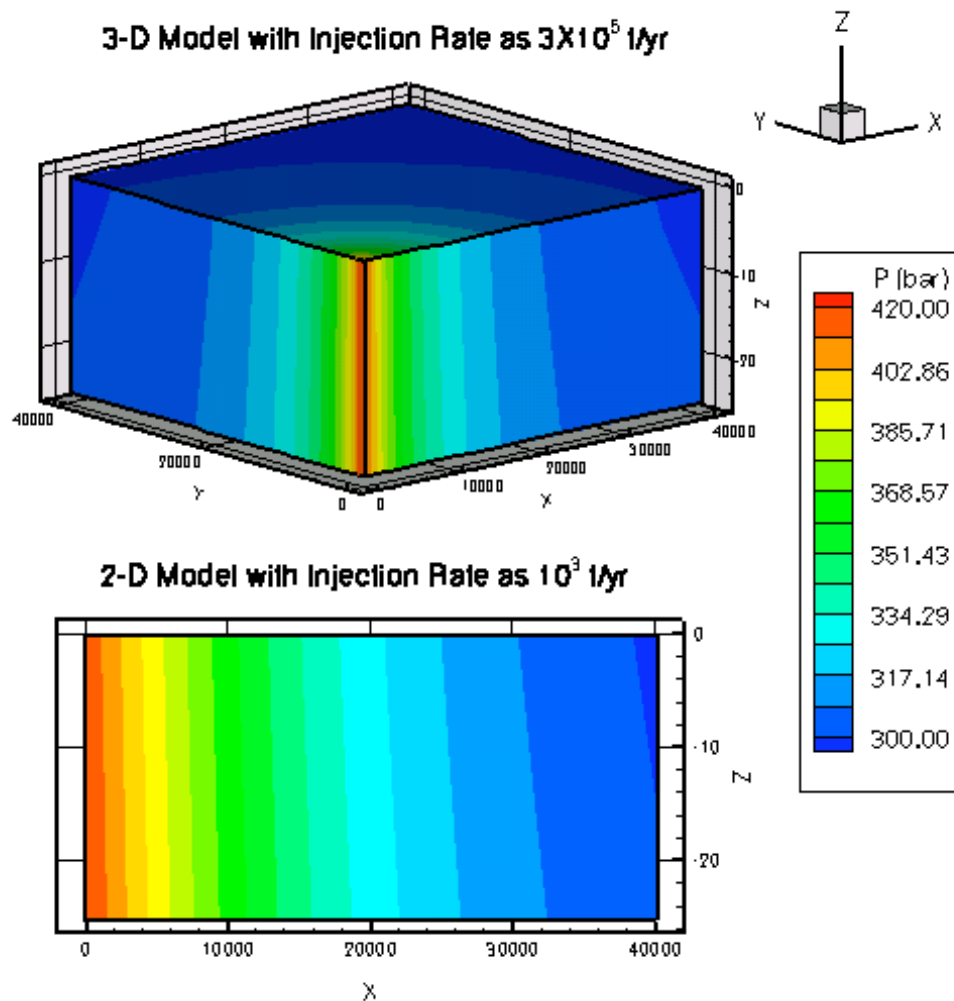


Figure 2. Comparison of 3-D and 2-D simulations of pressure fields generated by the injection of supercritical CO_2 at $\text{CO}_2 = 3 \times 10^5$ ton/year and 10^3 ton/year, respectively.

2-D Reactive-Transport Simulation

In our reactive-transport simulation, 10^3 tons/year of supercritical CO_2 is injected into the 2-D slice (25 m x 50 x 80 km) with an average permeability of 10 md. Figure 1 shows permeability distribution and Figures 3-6 show the calculated pressure, supercritical CO_2 , CO_2 (aq), and pH distributions as a function of time. The permeability field consists alternating layers of more and less permeability, where layers 1, 3, and 5 have higher permeability than layers 2, 4, and 6. Layer 5 has the highest permeability. In this realization, individual layers are more permeable towards the left of the injection than to the right.

It is known that the pressure front caused by injection of supercritical CO_2 moves at a much faster rate and over a much greater distance than the supercritical CO_2 . After 10 years of CO_2 injection, the over pressure is about 115 bars within 5 km of the well and grades to the background pressure between 30 and 40 km away from the well (Figure 3). While the CO_2 plume is restricted within 1.5 km of the injection well (Figure 4). The asymmetric pressure distribution is related to larger permeability to the left of the injection well than to the right of the well. In the post injection phase, the over pressure reduces to about 50 bars (reservoir pressure = 350 bars). Agreement of the pressure fields between the 3-D and 2-D simulations suggest that a CO_2 flux of 10^3 ton/year in a 2-D simulation would scale to an CO_2 injection of 3×10^5 ton/year in the field.

Examination of distribution of supercritical CO_2 in the pore space over time shows the importance of buoyancy and permeability at fairly low flux of CO_2 . Vertical and horizontal heterogeneity within the dolostone tend to distribute the supercritical CO_2 over a larger region than they would in a homogeneous reservoir. The time series clearly show that the highest saturations of supercritical CO_2 are stored in the most permeable layers (1, 3, and 5) with a preference towards the top of the reservoir in layer 1, followed by layer 3, despite the fact that layer 5 has the greatest permeability. Note that the distribution of supercritical CO_2 is asymmetric about the injection well and extends to greater extent to the left of the well where the permeability is higher than to the right of the well. During the post injection period between 10 and 20 years, buoyancy of supercritical CO_2 results in a greater distribution of CO_2 towards the permeable layers towards the top of the reservoir. In our simulation the injection well is open to the reservoir rock. Thus the well within the storage formation provides a high permeability pathway layers higher in the carbonate unit. If the well had been sealed within the formation, then it is likely that more CO_2 would be trapped between the lower permeable layers. This type of layering of supercritical CO_2 has also been observed seismically at Sleipner carbon sequestration site in the North Sea. At Sleipner, the layered storage of supercritical CO_2 is attributed to impermeable shale layers within the sandstone reservoir.

CO_2 (aq) and pH have similar plumes with a slightly larger footprint than CO_2 saturation (Figure 5 and 6). This is expected as dissolution of small amounts of CO_2 into the brine as carbonic acid yield large changes in dissolved CO_2 (aq) and pH. The CO_2 (aq) and pH plumes are concentrated along the injection pipe and into the most permeable layers during the first year of CO_2 injection. With continued injection the effect of permeability is only seen in the asymmetric

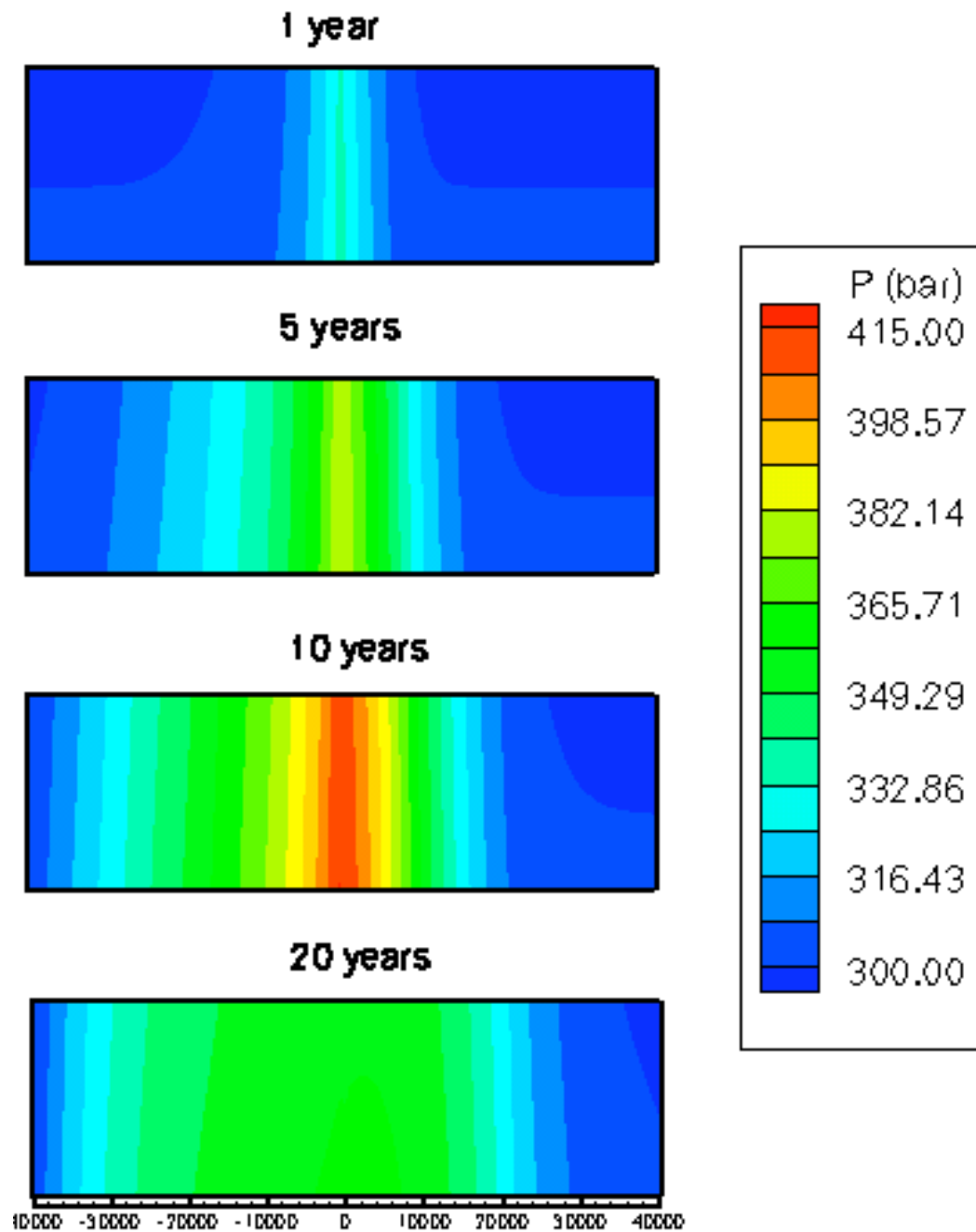


Figure 3. Pressure distribution resulting from injection of $\text{CO}_2 = 10^3$ ton/year. Injection period is from 0 to 10 years, post-injection period is from 10 to 20 years.

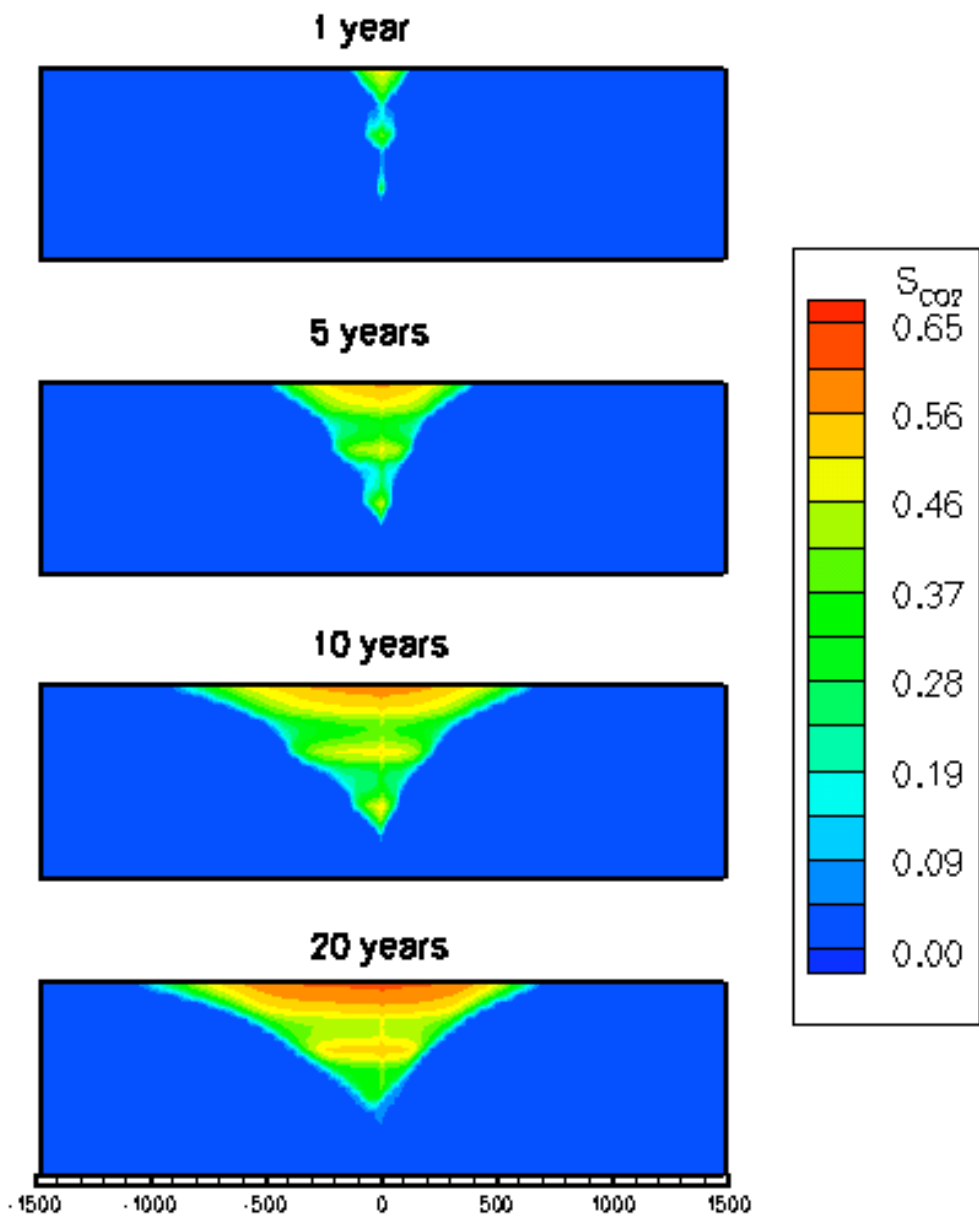


Figure 4. Fraction of supercritical CO₂ in the pore space resulting from injection of CO₂ = 10³ ton/year. Injection period is from 0 to 10 years, post-injection period is from 10 to 20 years.

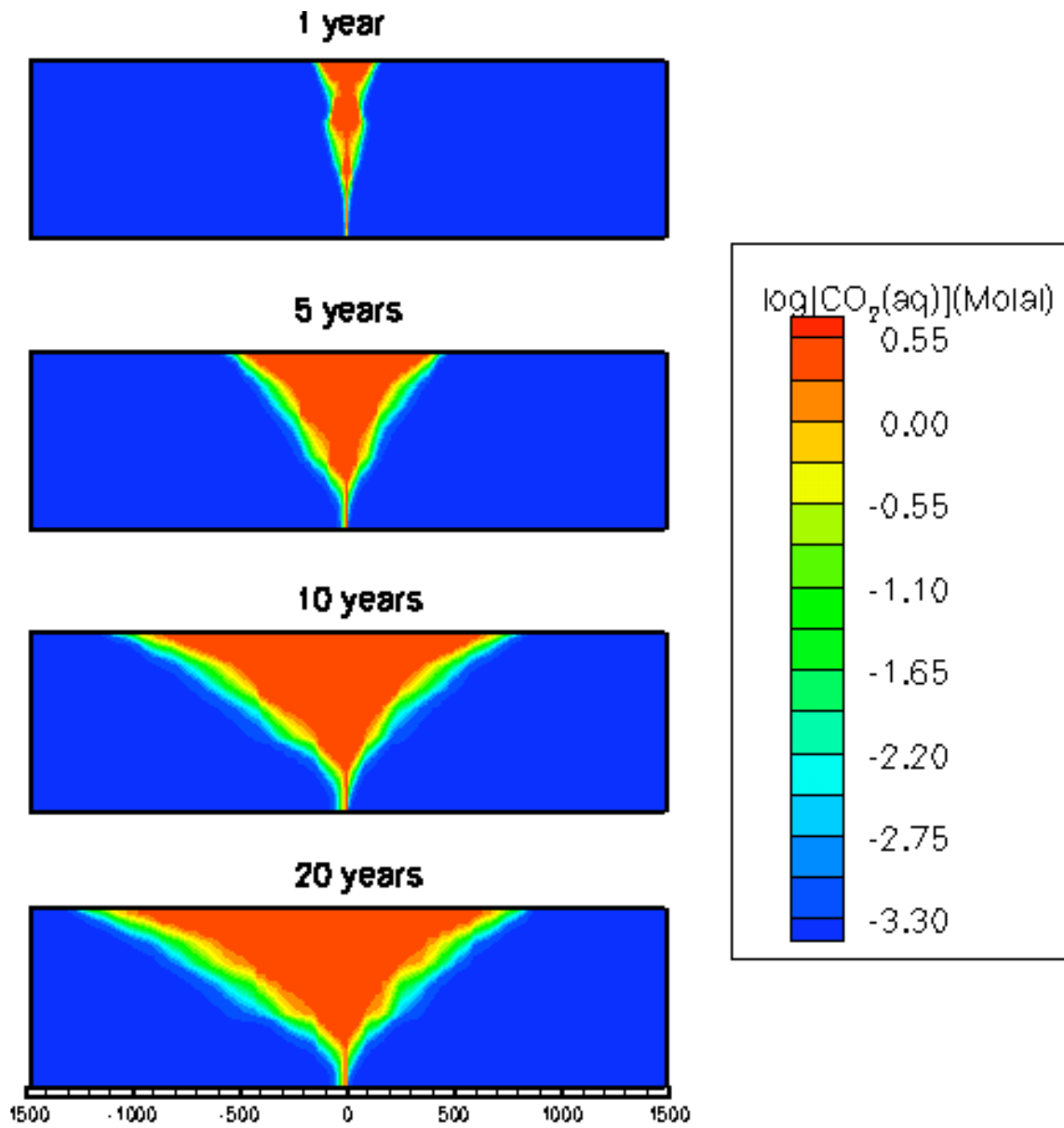


Figure 5. Concentration of CO₂(aq) in the pore space resulting from injection of CO₂ = 10³ ton/year. Injection period is from 0 to 10 years, post-injection period is from 10 to 20 years.

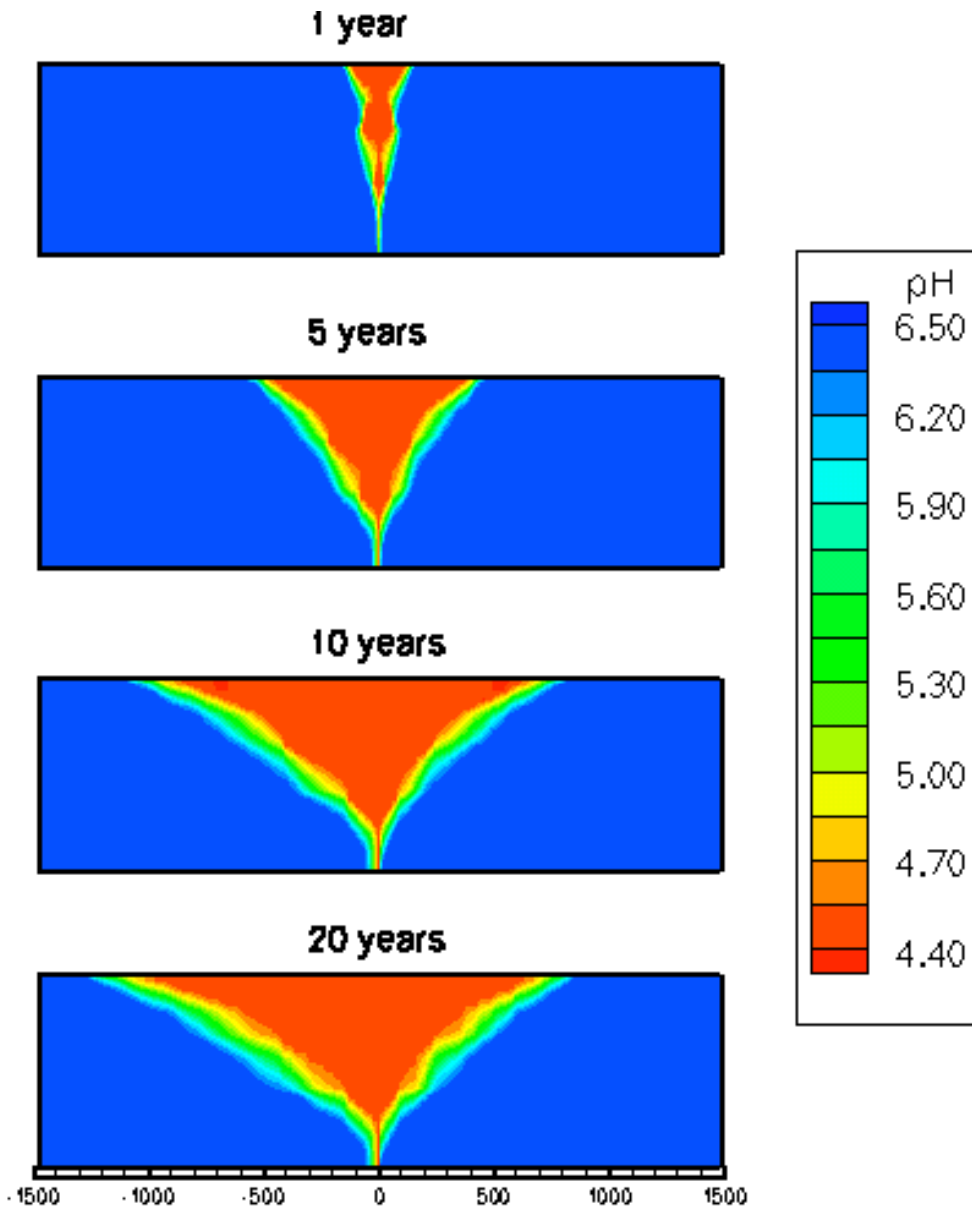


Figure 6. pH distribution resulting from injection of $\text{CO}_2 = 10^3$ ton/year. Injection period is from 0 to 10 years, post-injection period is from 10 to 20 years.

shape of the plume and the layering is lost as the partial pressure of CO_2 is high enough to yield pH near 4.5 even though the fraction of supercritical CO_2 is lower.

We expect changes in reservoir porosity and permeability to be minimal during injection and storage, because there is minimal mineral dissolution and precipitation of the carbonate geology. Figure 7 shows the percentage of the original amount of calcite and dolomite dissolved over the 20-year simulation near the injection well at the base of the dolostone reservoir. At this location the

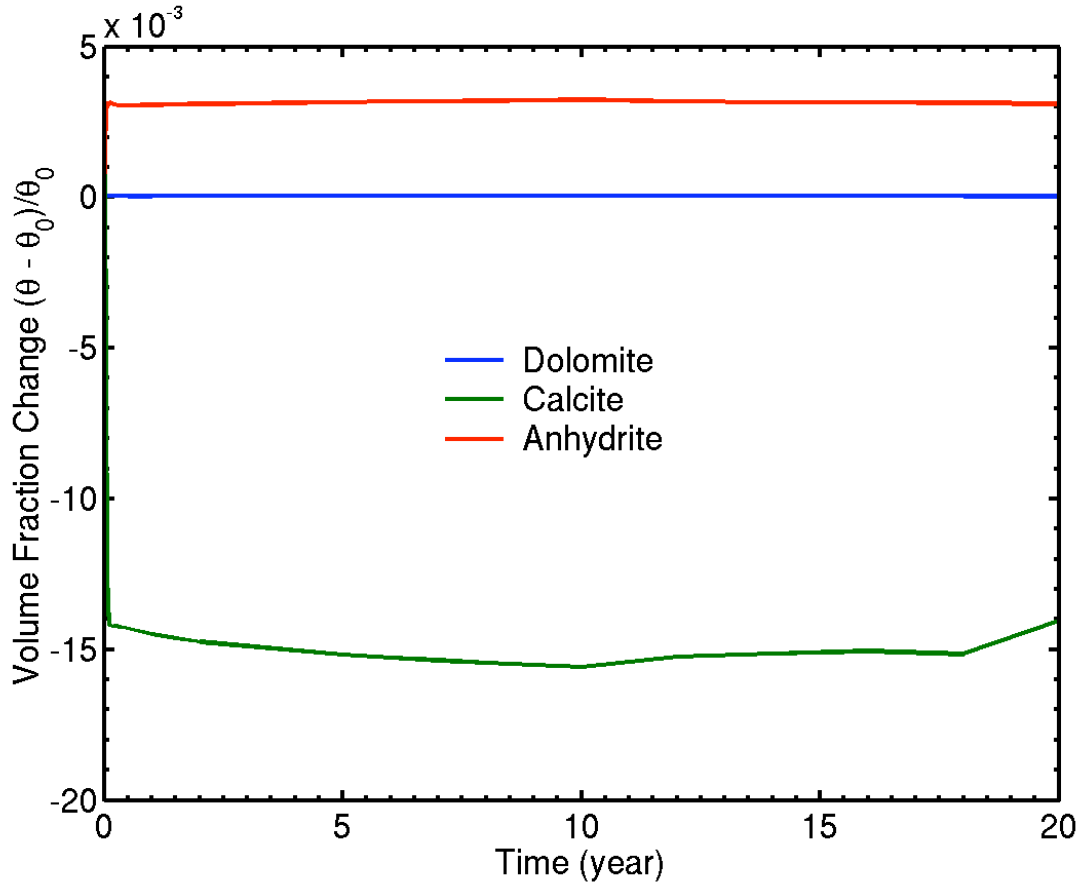


Figure 7. Change in mineral volume fraction of dolomite, calcite, and anhydrite caused by CO₂ injection into a carbonate rock with low permeability. Injection spans from 0 to 10 years. The location is near the injection well which experiences the most acid conditions over the run.

reservoir rock (98% dolomite, 1% calcite and 1% anhydrite) reacts with acidified brine (pH 4.45) during the injection and post injection phases. Dolomite dissolution is about 3 orders of magnitude slower than that of calcite. As a result the amount of dolomite dissolved is negligible and is on the order of the uncertainty in the numerical simulations. The amount of calcite dissolution is also quite small. Dissolution of about 1.5% of the initial volume of calcite in the rock (only 1%) increases the porosity by 0.015%. Some of calcium dissolved from calcite reacts with dissolved sulfate and forms anhydrite. Again the absolute amount is too small to impact porosity and permeability. A 0.3 % increase in the volume of anhydrate would reduce porosity by 0.003%.

Suitability of CO₂ injection into poorly permeable carbonate geology in the Ordos Basin for geologic storage

The preliminary simulations suggest that carbonate geology within the Ordos Basin is suitable for carbon sequestration. Firstly, heterogeneity within the reservoir creates higher storage capacity because the CO₂ is stored between the more impermeable layers and does not simply rise to the top of the formation, as it would in a more permeable and homogeneous formation. Secondly, the permeability structure or heterogeneity will not be destroyed by the acidity of the injected CO₂, because very small amounts of the carbonate minerals must dissolve to achieve equilibrium (in the absence of SO₂ contaminants, Knauss et al., 2002). Once the brines are in equilibrium no additional mineral dissolution is expected to occur. This is distinct from carbonate permeability that is formed in karst environments. In karst environments, large volumes of carbonate poor groundwaters dissolve relatively large amounts dolostone or limestone geology over time. In the CO₂ storage environment, the brine is saturated with respect to supercritical CO₂ and the formation waters are assumed to have very slow flow rates. As a result the available pool of reactant brine is limited to the pore volume, which is small in the carbonate geology in the Ordos Basin. Although chemistry does not alter the porosity and permeability within the storage formation, it is possible the reactions in the cap rock may play a more important role and that they may effectively seal the formation (Johnson et al. 2005)

Successful storage in the Ordos Basin will need to evaluate the role of pressure on reservoir and cap rock geomechanical stability to ensure the proper injection rate. We use an average permeability of 10 md in the storage formation. This is done in part to simulate a reasonable CO₂ injection rate and reasonable pressure fields. Simulations conducted a lower permeability or high flux yielded grossly high pressures that would surely damage reservoir and its cap rock (data not shown). It is also very important to measure the rock properties at the storage location well enough to make adequate predictions of storage over time. This includes parameters such as the likelihood of fracture permeability in addition to the pore scale permeability. We also strongly recommend that simulations for a specific site be conducted in 3-D to avoid potential artifacts from boundary conditions.

References

1. Buscheck TA, Glascoe LG, Lee KH, Gansemer J, Sun Y, Mansoor K: **Validation of the Multiscale Thermohydrologic Model used for analysis of a proposed repository at Yucca Mountain.** *J. Contaminant Hydrology* 2003, **62-3**:421-440.
2. Carroll, S., Hao, Y, Aines, R: **Geochemical detection of CO₂ in dilute aquifers.** *Geochemical Transactions* 2008, submitted.
3. Glassley WE, Nitao JJ, Grant CW: **Three-dimensional spatial variability of chemical properties around a monitored waste emplacement tunnel.** *J. Contaminant Hydrology* 2003 **62-63**: 495-507.
4. Greenberg, J. P., and Møller, N: **The prediction of mineral solubilities in natural waters: A chemical equilibrium model for the Na-K-Ca-Cl-SO₄-H₂O system to high concentration from 0 to 250°C.** *Geochimica et Cosmochimica Acta* 1989, 53: 2503-2518.
5. Helgeson, H. C.: **Thermodynamics of hydrothermal systems at elevated temperatures and pressures.** *American Journal of Science* 1969, 267: 729-804.
6. IPCC Intergovernmental Panel on Climate Change: 2007 web site <http://www.ipcc.ch/>
7. IEA International Energy Agency: *Greenhouse Gas R&D Programme* 2007. <http://www.ieagreen.org.uk/>
8. Johnson, J. W., Oelkers, E. H., and Helgeson, H. C: **SUPCRT92: A software package for calculating the standard molal thermodynamic properties of minerals, gases, aqueous species, and reactions from 1 to 5000 bars and 0° to 1000°C.** *Computers and Geosciences* 1992, 18:899-947.
9. Johnson JW, Nitao JJ, Knauss KG: **Reactive transport modeling of CO₂ storage in saline aquifers to elucidate fundamental processes, trapping mechanisms and sequestration partitioning.** In: *Geological Storage of Carbon Dioxide*. Edited by SJ Baines, RH Worden. *Geological Society, London, Special Publications* 2004, **223**: 107-128.
10. Johnson JW, Nitao JJ, Morris JP: **Reactive transport modeling of cap-rock integrity during natural and engineered CO₂ storage.** In *Carbon Dioxide Capture for Storage in Deep Geologic Formations*. Edited by D. C. Thomas and S. M. Benson: 2005, **2**: 787-813.
11. Knauss, K. G., Johnson, J. W., Steefel, C. I: **Evaluation of the impact of CO₂, co-contaminant gas, aqueous fluid and reservoir rock interactions on the geologic sequestration of CO₂.** *Chemical Geology* 2005, 217:339-350.
12. Nitao JJ: **Reference Manual for the NUFT Flow and Transport Code, Version 2.0.** UCRL-MA-130651. Lawrence Livermore National Laboratory, Livermore, CA, 1998

13. Palandri, J.L., Kharaka, Y.K: **A Compilation of Rate Parameters of Water-Mineral Interaction Kinetics for Application to Geochemical Modeling**. Open File Report 2004-1068, U.S. Department of the Interior, U.S. Geological Survey, 64 p
14. Petroleum Geology of Ordos Basin: A Synopsis on Petroleum Geology of China, V. 12.
15. Wang, B. and Al-Aasm, I. S: **Karst-controlled diagenesis and reservoir development: Example from the Ordovician main reservoir carbonate rocks on the eastern margin of the Ordos basin, China**, *AAPG Bulletin* 2002, 86:1639–1658
16. Wolery, T. J. 1992. *EQ3/6, A Software Package for Geochemical Modeling of Aqueous Systems: Package Overview and Installation Guide (Version 7.0)*. UCRL-MA-110662-PT-I, Lawrence Livermore National Laboratory, Livermore, California.
17. Wolery, T. J. 1992. *EQ3NR, A Computer Program for Geochemical Aqueous Speciation-Solubility Calculations: Theoretical Manual, User's Guide, and Related Documentation (Version 7.0)*. UCRL-MA-110662-PT-III, Lawrence Livermore National Laboratory, Livermore, California.
18. Wolery, T. J., and Daveler, S. A. 1992. *EQ6, A Computer Code for Reaction-Path Modeling of Aqueous Geochemical Systems (Version 7.0): Theoretical Manual, User's Guide, and Related Documentation*. UCRL-MA-110662-PT-IV, Lawrence Livermore National Laboratory, Livermore, California.